

Smart meta-superconductor MgB₂ constructed by inhomogeneous phase of luminescent nanocomposite

Yongbo Li, Honggang Chen, Mingzhong Wang, Longxuan Xu and Xiaopeng Zhao*

Smart Materials Laboratory, Department of Applied Physics, Northwestern Polytechnical University, Xi'an 710072, China; lybo2010@foxmail.com (Y.L.); 2017100698@mail.nwpu.edu.cn (H.C.); wangmingzhongsuper@163.com (M.W.); 554822887@qq.com (L.X.)

*Correspondence: xpzhao@nwpu.edu.cn (X.Z.)

Abstract

On the basis of the idea that the injecting energy will improve the conditions for the formation of Cooper pairs, a smart meta-superconductor (SMSC) was prepared by doping inhomogeneous phase of luminescent nanocomposite Y₂O₃:Eu³⁺/Ag, which has the strong luminescence characteristic, in MgB₂ to improve the superconducting transition temperature (T_C) of the MgB₂-based superconductor. Two types of Y₂O₃:Eu³⁺/Ag with different sizes were prepared and marked as m-Y₂O₃:Eu³⁺/Ag and n-Y₂O₃:Eu³⁺/Ag. MgB₂ SMSC was prepared through an ex situ process. Results show that when the inhomogeneous phase content was fixed at 2.0 wt.%, the T_C of MgB₂ SMSC increased initially then decreased with the increase in the Ag content in the dopant. When the Ag content accounted for 5 wt.% of the inhomogeneous phase weight, the T_C of MgB₂ SMSC was 37.2–38.0 K, which was similar to that of pure MgB₂. Meanwhile, the T_C of MgB₂ SMSC doped with n-Y₂O₃:Eu³⁺/Ag increased initially then decreased basically with the increase in the content of n-Y₂O₃:Eu³⁺/Ag, in which Ag accounted for 5 wt.% of the inhomogeneous phase. The T_C of MgB₂ SMSC doped with 0.5 wt.% n-Y₂O₃:Eu³⁺/Ag was 37.6–38.4 K, which was 0.4 K higher than that of pure MgB₂. It is thought that the doping inhomogeneous phase of luminescent nanocomposite into the superconductor is a new means to improve the T_C of SMSC.

Keywords: MgB₂; smart meta-superconductor; luminescent nanocomposite; inhomogeneous phase; Y₂O₃:Eu³⁺/Ag

Introduction

Improving the superconducting critical transition temperature of materials is an important scientific and technical problem in condensed matter physics and materials science. Recently, Fausti et al. [1] used mid-infrared femtosecond pulses to transform non-superconducting La_{1.675}Eu_{0.2}Sr_{0.125}CuO₄ into a transient 3D superconductor. A similar method was also applied to investigate YBa₂Cu₃O_{6.5} [2] and K₃C₆₀ [3,4], and good experimental results were achieved. Ye et al.

have reported the observation of field-induced superconductivity of ZrNCl and MoS₂ by quasi-continuous electrostatic carrier doping achieved by combining liquid and solid gating [5,6]. Drozdov et al. [7] reported conventional superconductivity at 203 K under high pressure in a sulfur hydride system. Adu et al. [8] increased the T_C of commercial “dirty” MgB₂ by conducting non-substitutional hole-doping of the MgB₂ structure using minute, single-wall carbon nanotube inclusions. In accordance with homogeneous system theory [9], Smolyaninov et al. [10-12] stated that a superconducting metamaterial with an effective dielectric response function that is less and approximately equal to zero may exhibit high T_C , and they verified this theory in their subsequent experiments. Recently, Cao et al. [13,14] investigated correlated insulator behavior at half-filling in magic-angle graphene superlattices and reported the realization of intrinsic unconventional superconductivity in a 2D superlattice created by stacking two sheets of graphene that are twisted relative to each other at a small angle. Another important method for studying superconductivity is the topological superconductors [15-20], which have attracted great attention in condensed matter physics. However, obtaining a practical superconductor with high T_C remains difficult.

The superconductivity of MgB₂ was discovered in 2001 [21]. MgB₂ is a promising material with large-scale applications because of its excellent superconducting properties and simple crystal structure [22-27]. Considering that the T_C of MgB₂ is close to the McMillan temperature limit [28,29], developing an effective experimental method to improve the T_C of MgB₂ is beneficial to its practical application and to the understanding of the superconducting mechanism. Chemical doping is a simple, effective, commonly used method to change the T_C of superconducting materials. However, many experimental results have confirmed that conventional chemical doping decreases the T_C of MgB₂ [30-36]. To date, no effective method has been developed to improve the T_C of MgB₂. The use of metamaterial structures to achieve special properties is an important method developed in recent decades [37-41], and it provides a new approach to improve the T_C of superconducting materials.

On the basis of metamaterials, our group investigated the effects of ZnO electroluminescent (EL) material doping on the superconductivity of BSCCO in 2007 and attempted to change the T_C of this superconductor [42]. Meanwhile, it is proposed that the combination of chemical doping and EL excitement, that is, doping EL materials in superconducting materials to form a meta structure, may be an effective method to improve the T_C of superconductors [43]. On the basis of these results, a smart meta-superconductor (SMSC) model for improving the T_C of materials has been proposed recently. In the model, the inhomogeneous phase is used to inject energy through its EL under the external field to strengthen the Cooper pairs, thereby achieving the purpose of changing the T_C . Zhang et al. [44] prepared MgB₂ doped with Y₂O₃:Eu³⁺ particles through an in situ process. Tao et al. [45] prepared MgB₂ doped with Y₂O₃:Eu³⁺ nanorods with different EL intensities through an ex

situ process. Their results indicated that doping EL materials is favorable for the improvement of T_C compared with conventional doping, which always reduces the superconducting transition temperature of the sample. In addition, similar experimental results were obtained by replacing $Y_2O_3:Eu^{3+}$ with $Y_3VO_4:Eu^{3+}$ flakes [46]. Meanwhile, results also indicated that the T_C can be changed by adjusting the $Y_2O_3:Eu^{3+}$ concentration and EL exciting current [47].

In this paper, a smart meta-superconductor was prepared by doping inhomogeneous phase of luminescent nanocomposite $Y_2O_3:Eu^{3+}/Ag$, which has the strong luminescence characteristic, in MgB_2 to improve the T_C of the MgB_2 -based superconductor. This inhomogeneous phase of nanocomposite illuminator $Y_2O_3:Eu^{3+}/Ag$ was prepared by our group, its EL intensity is three times higher than that of $Y_2O_3:Eu^{3+}$ due to the composite illumination of electroluminescence and photoluminescence [48]. Two kinds of nanocomposite illuminator $Y_2O_3:Eu^{3+}/Ag$ with different sizes, namely, micro $Y_2O_3:Eu^{3+}/Ag$ (m- $Y_2O_3:Eu^{3+}/Ag$) and nano $Y_2O_3:Eu^{3+}/Ag$ flakes (n- $Y_2O_3:Eu^{3+}/Ag$), are prepared. MgB_2 doped with a nanocomposite illuminator with high luminous intensity is prepared through an ex situ process [49]. The T_C of the MgB_2 -based superconductor is investigated by changing the Ag content in the inhomogeneous phase, the sizes of the inhomogeneous phase, and the doping concentration. The results indicate that the T_C of MgB_2 doped with 0.5 wt.% n- $Y_2O_3:Eu^{3+}/Ag$ is 37.6–38.4 K, which is 0.4 K higher than that of pure MgB_2 .

Experiment

1. Preparation of m- $Y_2O_3:Eu^{3+}/Ag$ and n- $Y_2O_3:Eu^{3+}/Ag$

Y_2O_3 (0.153 g) and Eu_2O_3 (0.012 g) were weighed and dissolved in a beaker with excess concentrated hydrochloric acid and subsequently heated and dried at 70 °C for 2 h to obtain a white precursor. One of the precursor was dissolved in 4 mL of deionized water to form a solution, and ammonium oxalate was added to it dropwise. The solution was subsequently stirred vigorously at 2 °C in a temperature-controlled water bath. A certain amount of $AgNO_3$ was added to the solution after been stirred for 30 min. After another 30 min of stirring, the pH value of the solution was adjusted to 9–10 by adding NaOH. The final solution, designated as solution A, was obtained after another 30 min of stirring. Another precursor was also prepared into solution with 24 mL benzyl alcohol. Octylamine (4 mL) was added dropwise to the solution, which was subsequently stirred for 1 h. Afterward, a certain amount of $AgNO_3$ was added to the solution. After stirring for another hour, another solution was obtained and designated as solution B. Solutions A and B were then transferred to two reaction kettles, respectively. A hydrothermal reaction occurred at 160 °C for 24 h. The products were washed several times with deionized water and absolute ethanol and sintered at 800 °C for 2 h to form $Y_2O_3:Eu^{3+}/AgCl$. After illumination, the $Y_2O_3:Eu^{3+}/AgCl$ transformed into two kinds of luminescent $Y_2O_3:Eu^{3+}/Ag$ nanocomposite with different sizes and a certain amount of

Ag. The two luminescent nanocomposite materials were designated as m-Y₂O₃:Eu³⁺/Ag and n-Y₂O₃:Eu³⁺/Ag. Y₂O₃:Eu³⁺/Ag with different Ag contents was prepared by changing the AgNO₃ content. Meanwhile, similar method was applied to synthesize Y₂O₃ and Y₂O₃:Sm³⁺.

2. Preparation of MgB₂-based SMSC

At a certain ratio, commercial MgB₂ powder and the luminescent nanocomposite Y₂O₃:Eu³⁺/Ag were weighed and prepared into an alcohol solution. The two suspensions were sonicated for 20 min, then the dopant was added dropwise to MgB₂. After sonication for more than 20 min, the mixed solution was transferred to a culture dish. Subsequently, the culture dish was placed in a vacuum oven at 60 °C for 4 h to yield a black powder. The powder was pressed into a tablet and placed in a small tantalum container, which was annealed at 800 °C for 2 h in high-purity argon atmosphere. The MgB₂-based superconductor doped with luminescent nanocomposite materials of different sizes and Ag contents was synthesized to investigate the *T_C* of SMSC.

Results and discussion

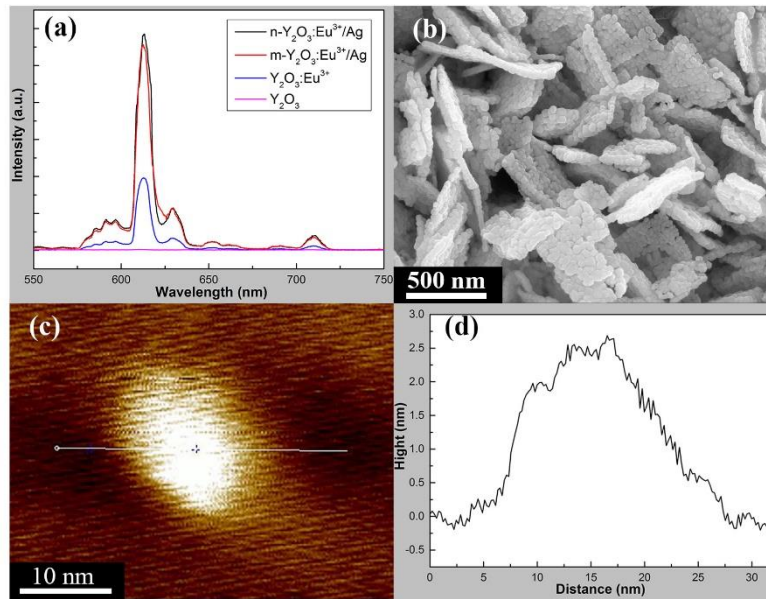


Figure 1. (a) EL spectra of Y₂O₃, Y₂O₃:Eu³⁺, m-Y₂O₃:Eu³⁺/Ag, and n-Y₂O₃:Eu³⁺/Ag; (b) SEM image of m-Y₂O₃:Eu³⁺/Ag; and (c-d) AFM image of n-Y₂O₃:Eu³⁺/Ag.

Figure 1a shows the EL spectra of Y₂O₃, Y₂O₃:Eu³⁺, m-Y₂O₃:Eu³⁺/Ag, and n-Y₂O₃:Eu³⁺/Ag. The Ag content of the luminescent nanocomposite materials was 5.0 wt.%. It shows that Y₂O₃ is a non-EL material and becomes a kind of EL material after the addition of a small amount of Eu element. The results also indicate that the EL intensity of the luminescent m-Y₂O₃:Eu³⁺/Ag nanocomposite and n-Y₂O₃:Eu³⁺/Ag is remarkably improved primarily due to the composite

luminescence of the electroluminescence of Eu^{3+} centric and the surface plasma-enhanced photoluminescence of Ag. Among the four dopants, $\text{n-Y}_2\text{O}_3:\text{Eu}^{3+}/\text{Ag}$ had the highest EL intensity. Figure 1b shows the SEM image of $\text{m-Y}_2\text{O}_3:\text{Eu}^{3+}/\text{Ag}$. The surface size and thickness of the $\text{m-Y}_2\text{O}_3:\text{Eu}^{3+}/\text{Ag}$ flake are approximately 300 nm and 30 nm, respectively. Figs. 1c–1d show AFM images of $\text{n-Y}_2\text{O}_3:\text{Eu}^{3+}/\text{Ag}$. The surface size of $\text{n-Y}_2\text{O}_3:\text{Eu}^{3+}/\text{Ag}$ was 20 nm, and its thickness was approximately 2.5 nm, which is much smaller than that of $\text{m-Y}_2\text{O}_3:\text{Eu}^{3+}/\text{Ag}$.

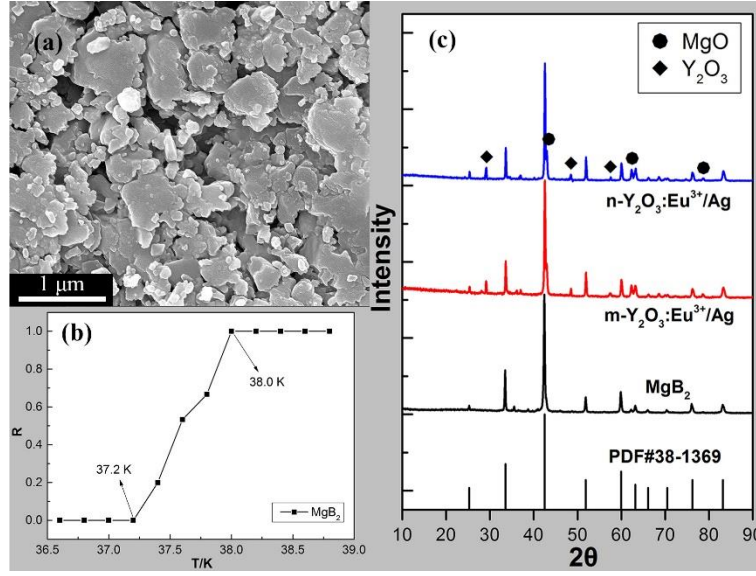


Figure. 2 (a) SEM image and (b) normalized temperature-dependent resistivity ($R-T$) curve of pure MgB_2 ; (c) XRD spectra of pure MgB_2 and MgB_2 doped with $\text{m-Y}_2\text{O}_3:\text{Eu}^{3+}/\text{Ag}$ and $\text{n-Y}_2\text{O}_3:\text{Eu}^{3+}/\text{Ag}$.

Figure 2a shows the SEM image of pure MgB_2 . The size of the MgB_2 particle was approximately 0.1–1 μm . The T_C of the samples was determined based on the $R-T$ curve, which was measured using a four-probe method in a liquid helium cryogenic system developed by the Advanced Research Systems Company. Figure 2b shows the normalized $R-T$ curve of pure MgB_2 and indicates that the onset temperature (T_c^{on}) and offset temperature (T_c^{off}) [50,51] of pure MgB_2 were 38.0 and 37.2 K, respectively. The superconducting transition width (ΔT) of pure MgB_2 was 0.8 K. Figure 2c shows the XRD spectra of pure MgB_2 and partially doped samples, in which the standard card of MgB_2 (PDF#38-1369) is demonstrated using black vertical lines. The results showed that the XRD spectrum of pure MgB_2 (black curve) matched the standard card of MgB_2 well, except for the inevitable small amount of the MgO phase [52–55]. The red and blue curves represent the XRD spectra of MgB_2 doped with 2.0 wt.% $\text{m-Y}_2\text{O}_3:\text{Eu}^{3+}/\text{Ag}$ and 2.0 wt.% $\text{n-Y}_2\text{O}_3:\text{Eu}^{3+}/\text{Ag}$, respectively. The Ag content was 5.0 wt.% of the dopant weight. The main phase of the doped samples was MgB_2 . Moreover, apart from a small amount of the MgO phase, the Y_2O_3 phase was also found in the XRD spectra of the doped samples. The XRD spectra of the other doped samples were similar.

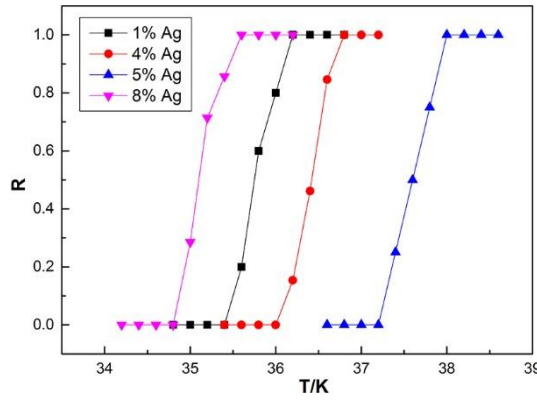


Figure 3. Normalized R - T curves of MgB_2 doped with 2.0 wt.% $\text{m-Y}_2\text{O}_3:\text{Eu}^{3+}/\text{Ag}$ with different Ag contents.

Figure 3 shows the normalized R - T curves of MgB_2 doped with $\text{m-Y}_2\text{O}_3:\text{Eu}^{3+}/\text{Ag}$ with different Ag contents. On the basis of the results of our previous study [45,46], the content of $\text{m-Y}_2\text{O}_3:\text{Eu}^{3+}/\text{Ag}$ in the four samples was fixed at 2.0 wt.%. The Ag contents of $\text{m-Y}_2\text{O}_3:\text{Eu}^{3+}/\text{Ag}$ in the four samples were 1 wt.%, 4 wt.%, 5 wt.%, and 8 wt.%, as shown in the figure, and their T_C values were 34.8–35.6, 36.0–36.8, 37.2–38.0, and 34.8–35.6 K, respectively. The T_C of the doped samples initially increased then decreased with the increase in Ag content. Meanwhile, the corresponding doped sample had the highest T_C when the concentration of $\text{m-Y}_2\text{O}_3:\text{Eu}^{3+}/\text{Ag}$ was fixed at 2.0 wt.% and the Ag content of $\text{m-Y}_2\text{O}_3:\text{Eu}^{3+}/\text{Ag}$ was 5 wt.%, which is equal to that of pure MgB_2 . The experimental results are similar to those of our previous studies, that is, doping EL materials may improve T_C in several cases compared with conventional doping, which always reduces the T_C of the sample. As a dopant, $\text{m-Y}_2\text{O}_3:\text{Eu}^{3+}/\text{Ag}$ exerts an impurity effect that decreases T_C . Meanwhile, as an EL material, $\text{m-Y}_2\text{O}_3:\text{Eu}^{3+}/\text{Ag}$ exerts an EL exciting effect that increases T_C [45,46]. An obvious competitive relationship exists between the impurity effect and the EL exciting effect. The final T_C of the samples increased when the EL exciting effect was fully utilized and the impurity effect was minimized.

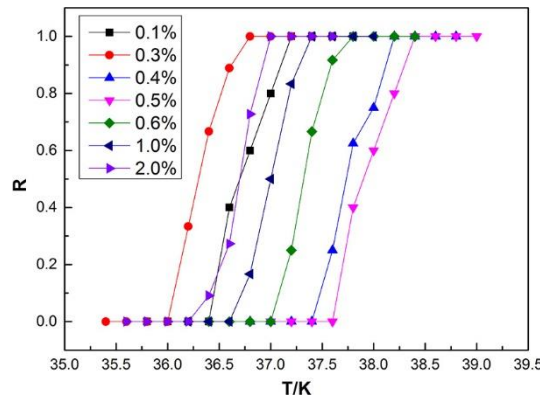


Figure 4. Normalized R - T curves of MgB_2 doped with $\text{n-Y}_2\text{O}_3:\text{Eu}^{3+}/\text{Ag}$.

Figure 4 shows the normalized R - T curves of MgB_2 doped with 0.1–2.0 wt.% $\text{n-Y}_2\text{O}_3\text{:Eu}^{3+}/\text{Ag}$. Ag concentration was fixed at 5.0 wt.% of the weight of $\text{n-Y}_2\text{O}_3\text{:Eu}^{3+}/\text{Ag}$. It can be seen that T_C of MgB_2 doped with $\text{n-Y}_2\text{O}_3\text{:Eu}^{3+}/\text{Ag}$ initially decreased, increased, then decreased again with the increase in doping concentration. A too low or too high doping concentration reduces T_C , which is similar to the finding of our previous study. When the doping concentration was in a low range, T_C decreased with the increase in doping concentration due to the dominance of the impurity effect of the dopant, which is similar to the results of conventional doping. The EL exciting effect of the dopant dominated with the further increase in doping concentration, resulting in the increase in T_C . The samples doped with 0.5 wt.% $\text{n-Y}_2\text{O}_3\text{:Eu}^{3+}/\text{Ag}$ had the highest T_C of 37.6–38.4 K, which is 0.4 K higher than that of pure MgB_2 . However, the impurity effect of the dopant dominated when the doping concentration increased to a high range, which led to a low T_C . These results indicate that doping luminescent nanocomposite materials effectively adjusts and improves T_C at an appropriate doping concentration.

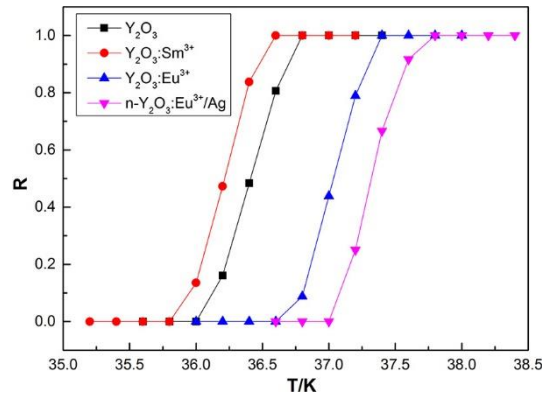


Figure 5. Normalized R - T curves of MgB_2 doped with Y_2O_3 , $\text{Y}_2\text{O}_3\text{:Sm}^{3+}$, $\text{Y}_2\text{O}_3\text{:Eu}^{3+}$, and $\text{n-Y}_2\text{O}_3\text{:Eu}^{3+}/\text{Ag}$.

MgB_2 doped with non-EL materials Y_2O_3 and $\text{Y}_2\text{O}_3\text{:Sm}^{3+}$ were synthesized to prove the conclusions above. Figure 5 shows the normalized R - T curves of MgB_2 doped with Y_2O_3 , $\text{Y}_2\text{O}_3\text{:Sm}^{3+}$, $\text{Y}_2\text{O}_3\text{:Eu}^{3+}$, and $\text{n-Y}_2\text{O}_3\text{:Eu}^{3+}/\text{Ag}$. The doping concentration was fixed at 0.6 wt.%, and the Ag content in $\text{n-Y}_2\text{O}_3\text{:Eu}^{3+}/\text{Ag}$ was 5.0 wt.%. Results indicated that T_C of MgB_2 doped with non-EL materials Y_2O_3 or $\text{Y}_2\text{O}_3\text{:Sm}^{3+}$ was much lower than that of pure MgB_2 , which is different from MgB_2 doped with EL materials at the same concentration. MgB_2 doped with EL materials at the same concentration. MgB_2 doped with $\text{Y}_2\text{O}_3\text{:Eu}^{3+}$ increased to 36.6–37.4 K due to the EL exciting effect. Meanwhile, MgB_2 doped with the luminescent $\text{n-Y}_2\text{O}_3\text{:Eu}^{3+}/\text{Ag}$ nanocomposite further increased to 37.0–37.8 K. The results show that doping EL materials facilitates an increase in T_C in several cases compared with conventional doping, which always reduces the T_C of the sample. Meanwhile, luminescent $\text{Y}_2\text{O}_3\text{:Eu}^{3+}/\text{Ag}$ nanocomposite materials increase the T_C of MgB_2 due to the strong EL intensity.

The results in Figure 4 show that the optimum concentration of $\text{n-Y}_2\text{O}_3\text{:Eu}^{3+}/\text{Ag}$ is 0.5 wt.%,

which is lower than the value in our previous study [44–46] due to the small size of n-Y₂O₃:Eu³⁺/Ag. The disadvantages caused by the impurity effect can be reduced if luminescent nanocomposite materials have a small size and are relatively evenly distributed in the sample. Moreover, the ΔT of commercial MgB₂ in our previous study [46] was too large to accurately determine the influence of the inhomogeneous phase on T_C . In the current study, a new kind of commercial MgB₂ with a small ΔT of 0.8 K was used, and we obtained a similar conclusion, which further proves the effectiveness of this method.

Conclusion

On the basis of the idea that the injecting energy will improve the conditions for the formation of Cooper pairs, a smart meta-superconductor was prepared by doping inhomogeneous phase of luminescent nanocomposite Y₂O₃:Eu³⁺/Ag in MgB₂ to improve the T_C of the MgB₂-based superconductor. Two types of Y₂O₃:Eu³⁺/Ag with different sizes were prepared and marked as m-Y₂O₃:Eu³⁺/Ag and n-Y₂O₃:Eu³⁺/Ag. MgB₂ SMSC was prepared through an ex situ process. SEM and AFM images indicated that the surface size and thickness of m-Y₂O₃:Eu³⁺/Ag are approximately 300 nm and 30 nm, which are 20 nm and 2.5 nm for n-Y₂O₃:Eu³⁺/Ag. The EL spectra showed that the EL intensity of luminescent nanocomposite Y₂O₃:Eu³⁺/Ag is three times higher than that of Y₂O₃:Eu³⁺. The T_C of MgB₂ SMSC was determined based on the measured R – T curve by using the four-probe method in a liquid helium cryogenic system. Results show that when the inhomogeneous phase content was fixed at 2.0 wt.%, the T_C of MgB₂ SMSC initially increased then decreased with the increase in the Ag content in the dopant. When the Ag content accounted for 5 wt.% of the inhomogeneous phase weight, the T_C of MgB₂ SMSC was 37.2–38.0 K, which was similar to that of pure MgB₂. Meanwhile, the T_C of MgB₂ SMSC doped with n-Y₂O₃:Eu³⁺/Ag increased initially then decreased basically with the increase in the content of n-Y₂O₃:Eu³⁺/Ag, in which Ag accounted for 5 wt.% of the inhomogeneous phase. The T_C of MgB₂ SMSC doped with 0.5 wt.% n-Y₂O₃:Eu³⁺/Ag was 37.6–38.4 K, which was 0.4 K higher than that of pure MgB₂. It is thought that the doping inhomogeneous phase of luminescent nanocomposite into the superconductor is a new means to improve the T_C of SMSC.

Funding: This work was supported by the National Natural Science Foundation of China for Distinguished Young Scholar under Grant No. 50025207.

References

1. Fausti, D.; Tobey, R.I.; Dean, N.; S.Kaiser; Dienst, A.; Hoffmann, M.C.; Pyon, S.; Takayama, T.; Takagi, H.; Cavalleri, A. Light-Induced Superconductivity in a Stripe-Ordered Cuprate. *Science* **2011**, *331*, 189–191.

2. Hu, W.; Kaiser, S.; Nicoletti, D.; Hunt, C.R.; Gierz, I.; Hoffmann, M.C.; Tacon, M.L.; Loew, T.; Keimer, B.; Cavalleri, A. Optically enhanced coherent transport in $\text{YBa}_2\text{Cu}_3\text{O}_{6.5}$ by ultrafast redistribution of interlayer coupling. *Nat. Mater.* **2014**, *13*, 705-711.
3. Mitrano, M.; Cantaluppi, A.; Nicoletti, D.; Kaiser, S.; Perucchi, A.; Lupi, S.; Di Pietro, P.; Pontiroli, D.; Ricco, M.; Clark, S.R.; Jaksch, D.; Cavalleri, A. Possible light-induced superconductivity in K_3C_{60} at high temperature. *Nature* **2016**, *530*, 461-464.
4. Cantaluppi, A.; Buzzi, M.; Jotzu, G.; Nicoletti, D.; Mitrano, M.; Pontiroli, D.; Ricco, M.; Perucchi, A.; Di Pietro, P.; Cavalleri, A. Pressure tuning of light-induced superconductivity in K_3C_{60} . *Nat. Phys.* **2018**, *14*, 837-841.
5. Ye, J.T.; Inoue, S.; Kobayashi, K.; Kasahara, Y.; Yuan, H.T.; Shimotani, H.; Iwasa, Y. Liquid-gated interface superconductivity on an atomically flat film. *Nat. Mater.* **2010**, *9*, 125-128.
6. Ye, J.T.; Zhang, Y.J.; Akashi, R.; Bahramy, M.S.; Arita, R.; Iwasa, Y. Superconducting Dome in a Gate-Tuned Band Insulator. *Science* **2012**, *338*, 1193-1196.
7. Drozdov, A.P.; Eremets, M.I.; Troyan, I.A.; Ksenofontov, V.; Shylin, S.I. Conventional superconductivity at 203 kelvin at high pressures in the sulfur hydride system. *Nature* **2015**, *525*, 73-76.
8. Ma, D.h.; Jayasingha, R.; Hess, D.T.; Adu, K.W.; Sumanasekera, G.U.; Terrones, M. Enhancing the superconducting temperature of MgB_2 by SWCNT dilution. *Physica C* **2014**, *497*, 43-48.
9. Kirzhnits, D.A.; Maksimov, E.G.; Khomskii, D.I. The description of superconductivity in terms of dielectric response function. *J. Low Temp. Phys.* **1973**, *10*, 79-93.
10. Smolyaninova, V.N.; Yost, B.; Zander, K.; Osofsky, M.S.; Kim, H.; Saha, S.; Greene, R.L.; Smolyaninov, I.I. Experimental demonstration of superconducting critical temperature increase in electromagnetic metamaterials. *Sci. Rep.* **2014**, *4*, 7321.
11. Smolyaninova, V.N.; Zander, K.; Gresock, T.; Jensen, C.; Prestigiacomo, J.C.; Osofsky, M.S.; Smolyaninov, I.I. Using metamaterial nanoengineering to triple the superconducting critical temperature of bulk aluminum. *Sci. Rep.* **2015**, *5*, 15777.
12. Smolyaninov, I.I.; Smolyaninova, V.N. Theoretical modeling of critical temperature increase in metamaterial superconductors. *Phys. Rev. B* **2016**, *93*,
13. Cao, Y.; Fatemi, V.; Demir, A.; Fang, S.; Tomarken, S.L.; Luo, J.Y.; Sanchez-Yamagishi, J.D.; Watanabe, K.; Taniguchi, T.; Kaxiras, E.; Ashoori, R.C.; Jarillo-Herrero, P. Correlated insulator behaviour at half-filling in magic-angle graphene superlattices. *Nature* **2018**, *556*, 80-84.
14. Cao, Y.; Fatemi, V.; Fang, S.; Watanabe, K.; Taniguchi, T.; Kaxiras, E.; Jarillo-Herrero, P. Unconventional superconductivity in magic-angle graphene superlattices. *Nature* **2018**, *556*, 43-50.
15. Qi, X.L.; Zhang, S.C. Topological insulators and superconductors. *Rev. Mod. Phys.* **2011**, *83*, 1057-1110.
16. Wang, Z.; Qi, X.L.; Zhang, S.C. Topological field theory and thermal responses of interacting topological superconductors. *Phys. Rev. B* **2011**, *84*, 014527.
17. Leijnse, M.; Flensberg, K. Introduction to topological superconductivity and Majorana fermions. *Semicond. Sci. Technol.* **2012**, *27*, 124003.
18. Schnyder, A.P.; Brydon, P.M. Topological surface states in nodal superconductors. *J. Phys.: Condens. Matter* **2015**, *27*, 243201.
19. Sato, M.; Ando, Y. Topological superconductors: a review. *Rep. Prog. Phys.* **2017**, *80*, 076501.
20. Fatemi, V.; Wu, S.; Cao, Y.; Brethau, L.; Gibson, Q.D.; Watanabe, K.; Taniguchi, T.; Cava, R.J.; Jarillo-Herrero, P. Electrically tunable low-density superconductivity in a monolayer topological

- insulator. *Science* **2018**, doi:10.1126/science.aar4642.
21. Nagamatsu, J.; Nakagawa, N.; Muranaka, T.; Zenitani, Y.; Akimitsu, J. Superconductivity at 39 K in magnesium diboride. *Nature* **2001**, *410*, 63-64.
 22. Buzea, C.; Yamashita, T. Review of the superconducting properties of MgB₂. *Supercond. Sci. Technol.* **2001**, *14*, R115-R146.
 23. Eisterer, M. Magnetic properties and critical currents of MgB₂. *Supercond. Sci. Technol.* **2007**, *20*, R47-R73.
 24. Vinod, K.; Varghese, N.; Syamaprasad, U. Superconductivity of MgB₂ in the BCS framework with emphasis on extrinsic effects on critical temperature. *Supercond. Sci. Technol.* **2007**, *20*, R31-R45.
 25. Xi, X.X. Two-band superconductor magnesium diboride. *Rep. Prog. Phys.* **2008**, *71*, 116501.
 26. Ma, Z.Q.; Liu, Y.C.; Cai, Q. The synthesis of lamellar nano MgB₂ grains with nanoimpurities, flux pinning centers and their significantly improved critical current density. *Nanoscale* **2012**, *4*, 2060-2065.
 27. Prikhna, T.A.; Eisterer, M.; Weber, H.W.; Gawalek, W.; Kovylaev, V.V.; Karpets, M.V.; Basyuk, T.V.; Moshchil, V.E. Nanostructural inhomogeneities acting as pinning centers in bulk MgB₂ with low and enhanced grain connectivity. *Supercond. Sci. Technol.* **2014**, *27*, 044013.
 28. Bardeen, J.; Cooper, L.N.; Schrieffer, J.R. Theory of Superconductivity. *Phys. Rev.* **1957**, *108*, 1175-1204.
 29. McMillan, W.L. Transition Temperature of Strong-Coupled Superconductors. *Phys. Rev.* **1968**, *167*, 331-344.
 30. Slusky, J.S.; Rogado, N.; Regan, K.A.; Hayward, M.A.; Khalifah, P.; He, T.; Inumaru, K.; Loureiro, S.M.; Haas, M.K.; Zandbergen, H.W.; Cava, R.J. Loss of superconductivity with the addition of Al to MgB₂ and a structural transition in Mg_{1-x}Al_xB₂. *Nature* **2001**, *410*, 343-345.
 31. Zhao, Y.G.; Zhang, X.P.; Qiao, P.T.; Zhang, H.T.; Jia, S.L.; Cao, B.S.; Zhu, M.H.; Han, Z.H.; Wang, X.L.; Gu, B.L. Effect of Li doping on structure and superconducting transition temperature of Mg_{1-x}Li_xB₂. *Physica C* **2001**, *361*, 91-94.
 32. Luo, H.; Li, C.M.; Luo, H.M.; Ding, S.Y. Study of Al doping effect on superconductivity of Mg_{1-x}Al_xB₂. *J. Appl. Phys.* **2002**, *91*, 7122-7124.
 33. Cava, R.J.; Zandbergen, H.W.; Inumaru, K. The substitutional chemistry of MgB₂. *Physica C* **2003**, *385*, 8-15.
 34. Kazakov, S.M.; Puzniak, R.; Rogacki, K.; Mironov, A.V.; Zhigadlo, N.D.; Jun, J.; Soltmann, C.; Batlogg, B.; Karpinski, J. Carbon substitution in MgB₂ single crystals: Structural and superconducting properties. *Phys. Rev. B* **2005**, *71*, 024533.
 35. Bianconi, A.; Busby, Y.; Fratini, M.; Palmisano, V.; Simonelli, L.; Filippi, M.; Sanna, S.; Congiu, F.; Saccone, A.; Giovannini, M.; De Negri, S. Controlling the Critical Temperature in Mg_{1-x}Al_xB₂. *J. Supercond. Nov. Magn.* **2007**, *20*, 495-501.
 36. Monni, M.; Affronte, M.; Bernini, C.; Di Castro, D.; Ferdeghini, C.; Lavagnini, M.; Manfrinetti, P.; Orecchini, A.; Palenzona, A.; Petrillo, C.; Postorino, P.; Sacchetti, A.; Sacchetti, F.; Putti, M. Role of charge doping and lattice distortions in codoped Mg_{1-x}(AlLi)_xB₂ compounds. *Physica C* **2007**, *460-462*, 598-599.
 37. Liu, H.; Zhao, X.P.; Yang, Y.; Li, Q.W.; Lv, J. Fabrication of Infrared Left - Handed Metamaterials via Double Template - Assisted Electrochemical Deposition. *Adv. Mater.* **2008**, *20*, 2050-2054.
 38. Qiao, Y.P.; Zhao, X.P.; Su, Y.Y. Dielectric metamaterial particles with enhanced efficiency of mechanical/electrical energy transformation. *J. Mater. Chem.* **2011**, *21*, 394-399.

39. Kurter, C.; Tassin, P.; Zhuravel, A.P.; Zhang, L.; Koschny, T.; Ustinov, A.V.; Soukoulis, C.M.; Anlage, S.M. Switching nonlinearity in a superconductor-enhanced metamaterial. *Appl. Phys. Lett.* **2012**, *100*, 121906.
40. Zhao, X.P. Bottom-up fabrication methods of optical metamaterials. *J. Mater. Chem.* **2012**, *22*, 9439-9449.
41. Ma, X.; Pu, M.; Li, X.; Guo, Y.; Gao, P.; Luo, X. Meta-Chirality: Fundamentals, Construction and Applications. *Nanomaterials* **2017**, *7*, 116.
42. Jiang, W.T.; Xu, Z.L.; Chen, Z.; Zhao, X.P. Introduce uniformly distributed ZnO nano-defects into BSCCO superconductors by nano-composite method. *J. Funct. Mater* **2007**, *38*, 157-160, in Chinese, available at <http://www.cnki.com.cn/Article/CJFDTOTAL-GNCL200701046.htm>.
43. Xu, S.H.; Zhou, Y.W.; Zhao, X.P. Research and Development of Inorganic Powder EL Materials. *Mater. Rev.* **2007**, *21*, 162-166, in Chinese, available at <http://www.cnki.com.cn/Article/CJFDTotal-CLDB2007S3048.htm>.
44. Zhang, Z.W.; Tao, S.; Chen, G.W.; Zhao, X.P. Improving the Critical Temperature of MgB₂ Superconducting Metamaterials Induced by Electroluminescence. *J. Supercond. Nov. Magn.* **2016**, *29*, 1159-1162.
45. Tao, S.; Li, Y.B.; Chen, G.W.; Zhao, X.P. Critical Temperature of Smart Meta-superconducting MgB₂. *J. Supercond. Nov. Magn.* **2017**, *30*, 1405-1411.
46. Li, Y.B.; Chen, H.G.; Qi, W.C.; Chen, G.W.; Zhao, X.P. Inhomogeneous Phase Effect of Smart Meta-Superconducting MgB₂. *J. Low Temp. Phys.* **2018**, *191*, 217-227.
47. Chen, H.G.; Li, Y.B.; Chen, G.W.; Xu, L.X.; Zhao, X.P. The Effect of Inhomogeneous Phase on the Critical Temperature of Smart Meta-superconductor MgB₂. *J. Supercond. Nov. Magn.* **2018**, *31*, 3175-3182.
48. Wang, M.Z.; Xu, L.X.; Chen, G.W.; Zhao, X.P. Topological luminophor Y₂O₃:Eu³⁺+Ag with high electroluminescence performance. *ACS Appl. Mat. Interfaces* (under review), arXiv:1810.03242 [cond-mat.mes-hall].
49. Zhao, X.P.; Li, Y.B.; Chen, H.G.; Chen, G.W. MgB₂-based superconductor constructed by inhomogeneous phase of topological illuminator and its preparation method. Chinese Patent 201810462942.X.
50. Kušević, I.; Marohnić, Ž.; E. Babić; Drobač, Đ.; Wang, X.L.; Dou, S.X. Flux pinning and critical currents in polycrystalline MgB₂. *Solid State Commun.* **2002**, *122*, 347-350.
51. Bhadauria, P.P.S.; Gupta, A.; Kishan, H.; Narlikar, A.V. Connectivity and critical current density of in-situ processed MgB₂ superconductors: Effect of excess Mg and non-carbon based additives. *J. Appl. Phys.* **2014**, *115*, 183905.
52. Eyidi, D.; Eibl, O.; Wenzel, T.; Nickel, K.G.; Giovannini, M.; Saccone, A. Phase analysis of superconducting polycrystalline MgB₂. *Micron* **2003**, *34*, 85-96.
53. Shi, Q.Z.; Liu, Y.C.; Gao, Z.M.; Zhao, Q. Formation of MgO whiskers on the surface of bulk MgB₂ superconductors during in situ sintering. *J. Mater. Sci.* **2007**, *43*, 1438-1443.
54. Ma, Z.Q.; Liu, Y.C.; Shi, Q.Z.; Zhao, Q.; Gao, Z.M. The improved superconductive properties of MgB₂ bulks with minor Cu addition through reducing the MgO impurity. *Physica C* **2008**, *468*, 2250-2253.
55. Singh, D.K.; Tiwari, B.; Jha, R.; Kishan, H.; Awana, V.P.S. Role of MgO impurity on the superconducting properties of MgB₂. *Physica C* **2014**, *505*, 104-108.